Pion-to-photon transition distribution amplitudes in the non-local chiral quark model

Piotr Kotko[†] **and Michał Praszałowicz**[‡]

M.Smoluchowski Institute of Physics,
Jagellonian University,
Reymonta 4, 30-059 Kraków, Poland.

We apply the non-local chiral quark model to study vector and axial pion-to-photon transition amplitudes that are needed as a nonperturbative input to estimate the cross section of pion annihilation into the real and virtual photon. We use a simple form of the non-locality that allows to perform all calculations in the Minkowski space and guaranties polynomiality of the TDA's. We note only residual dependence on the precise form of the cut-off function, however vector TDA that is symmetric in skewedness parameter in the local quark model is no longer symmetric in the non-local case. We calculate also the transition form-factors and compare them with existing experimental parametrizations.

1. Introduction

Exclusive processes involving hadrons factorize in the Bjorken limit into a hard cross section and a soft hadronic matrix element that cannot be calculated in perturbative QCD. Those matrix elements encode nonperturbative information on the hadronic structure. Recently Pire and Szymanowski [1] introduced new objects of this type that describe pion-to-photon $(\pi 2\gamma)$ transition in the presence of the $q\bar{q}$ operator that in the following will be denoted by Γ. Depending on the nature of Γ one can define vector or axial transition distribution amplitudes (VTDA or ATDA respectively). In their original work Pire an Szymanowski discussed hadron-antihadron scattering process $H\bar{H} \to \gamma^*\gamma$ where the virtual photon supplies the hard scale allowing for perturbative treatment, whereas the other photon is on mass-shell. As the simplest case, to avoid complications with spin or multiquark

---

[†] e-mail: kotko@th.if.uj.edu.pl
[‡] e-mail: michal@if.uj.edu.pl

bound states, one may take pions as initial hadrons. Although experimentally difficult to access [2], $\pi\pi$ scattering is of particular theoretical interest, since pions are Goldstone bosons of broken SU(2) chiral symmetry and their properties are to large extent determined by the symmetry (breaking) alone rather than by the complex phenomenon of confinement.

Indeed, there exists in the literature a variety of chiral models which involve both constituent quarks and pion degrees of freedom. In Ref.[3] Tiburzi used simple constituent quark model to discuss properties of the $\pi 2\gamma$ TDA's. Similar model with Pauli-Villars regularization has been recently used by Courtoy and Noguera [4] to calculate $\pi 2\gamma$ TDA's for different ranges of kinematical variables. Finally Ruiz Arriola and Broniowski [5] employed the Spectral Quark Model (SQM) for the same purpose.

One of the important ingredients of the low energy models is regularization. Even though $\pi 2\gamma$ TDA's are formally finite, regularization cannot be simply dropped out, since it defines the scale of applicability above which the models do not apply. In this paper we calculate $\pi 2\gamma$ TDA's in the semibosonized Nambu–Jona-Lasinio model known also as the Chiral Quark Model (χQM) with non-local regulator. This model has been previously used to calculate pion [6], pion and kaon [7] distribution amplitudes (DA) and generalized parton distributions (GPD) together with two-pion distribution amplitudes [8]. Direct comparison of local and non-local versions of the model allows to determine the influence of the non-local regulator. In most cases rather sharp curves obtained within the local model are smoothed down; also the endpoint behavior of various distributions is made continuous. This phenomenon is at best illustrated by the example of the pion distribution amplitude which in the local model is constant over the whole support, whereas the non-local regulator forces it to vanish in the endpoints [9, 10]. It is therefore of interest to investigate the role of the non-local regulator for the $\pi 2\gamma$ TDA's introduced above.

One has to remember that χQM, although devised to describe chiral physics of Goldstone bosons, has been widely used to incorporate baryons as chiral solitons both in local (for review see *e.g.* Ref.[11]) and non-local [12] cases. Generally the results of these studies show that the soliton ceases to exist for too small constituent quark mass M. The critical value of M depends on the details of the given model, however it is of the order of 300 MeV or a bit less. Typical values of M that fit well the hyperon spectrum may be as high as 420 MeV [13]. In the present paper we adopt two distinct values of M: 350 MeV and 225 MeV. The latter, as we shall se in Sect.6, fits well the slope of the $\pi 2\gamma$ transition form-factor. It is, however, excluded if one wants to describe baryons as chiral solitons.

Our results can be in short summarized as follows: it seems that $\pi 2\gamma$ TDA's are quite robust as far as different regularization schemes (including

no cut-off at all) are concerned. On the one hand this is a welcome feature for phenomenology, one can use them with large degree of confidence. On the other hand they cannot be used to distinguish between different models. However, as we shall discuss in Sect. 5.2, the ξ-symmetry of the VTDA is no longer present in the non-local model, and the results for $\xi < 0$ differ more from the results of the local model, than the ones for $\xi > 0$ (where ξ is the *skewedness* parameter to be defined in Sect. 4). We shall also see that the normalizations of VTDA and ATDA which are equal in the local model become different in the non-local case.

In the next section we shall discuss different chiral quark models existing in the literature in the context of $\pi 2\gamma$ TDA's. Subsequently in Sect. 3 we give a short overview of the non-local model used in the present paper. We shall work in a symmetric kinematics that is introduced in Sect. 4 together with the definitions of the TDA's in question. Calculations and results are presented in Sect. 5. We summarize and give our conclusions in Sect. 6. Technical details can be found in Appendices A–C.

2. Quark models and the transition amplitudes

In order to estimate transition amplitudes one may try to construct phenomenological ansatze that satisfy general conditions such as gauge invariance and anomaly structure, Lorentz invariance that in our case is equivalent to polynomiality, *etc.*. For special limiting cases these ansatze reduce to known form factors or structure functions (see *e.g.* Ref.[14], or in the context of $\pi 2\gamma$ TDA's Ref.[3]). Alternatively one may try to resort to some kind of nonperturbative calculations. Usually a good staring point is a constituent quark model where all nonperturbative effects are parametrized in terms of a constituent quark mass and a chirally invariant meson-quark coupling (Local Chiral Quark Model – LχQM). As quite useful first approximation such model has been used in Refs.[9, 10] to describe pion light cone distribution amplitude or two pion distribution amplitudes [15]. The results of the LχQM seem rather trivial. For example pion light cone distribution amplitude is constant and does not vanish in the endpoints [9, 6], similarly the isoscalar skewed pion distribution amplitude is just a superposition of the Θ functions [6]. While LχQM satisfies Ward identities, it violates Lorentz invariance by the necessary transverse UV cut-off.

Let us stress that the UV cut-off is not merely a regulator, on the contrary, it defines the applicability domain of the model that is clearly devised as low energy approximation to QCD. It should be therefore applied also to the quantities that are formally finite in this limit. However, as we shall shortly explain in some more detail, the explicit UV cut-off results in a violation of the polynomiality which is essential for the transition amplitudes

that are discussed in this paper. Clearly a more sophisticated regulator is needed.

One might expect that a more sophisticated regularization which preserves Lorentz invariance would result in a more realistic shape of the pion distribution amplitude. This is, however, not necessarily the case. Gauge invariant regulator is provided for example by the Spectral Quark Model (SQM) Refs.[16, 5], where the constituent quark mass M is traded for a spectral parameter ω, and all physical quantities are given in terms of integrals over $d\omega$ with some a priori unknown spectral density $\rho(\omega)$. Spectral density $\rho(\omega)$ must satisfy a number of relations that follow from the QCD Ward identities; explicit realizations of the model with explicit form of $\rho(\omega)$ are also known [16]. Although at first sight theoretically attractive, SQM yields phenomenological results that are very similar to the naive LχQM described above.

Similarly in Ref.[17] a Pauli-Villars regularized Nambu–Jona-Lasinio model was applied to calculate both pion distribution amplitude (DA) and parton distributions in the pseudoscalar mesons. Again pion DA at the input scale is given as a step function and does not vanish in the endpoints. Evidently a form factor in the quark-pion vertex is needed to "soften" the shape of the (generalized) distribution amplitudes.

An attractive and simple way out is provided by the Non-Local Chiral Quark Model (NLχQM) where the quark-pion coupling is given in terms of a momentum dependent constituent quark mass $M(p)$. For small p, $M(p) \to M \sim 350$ MeV, whereas for $p \to \infty$, $M(p) \to 0$. This suppression of large momenta (remember that the constituent quark mass $M(p)$ acts not only as a mass parameter in the propagators, but also – more importantly – as a quark-meson coupling) is enough to make the pion distribution amplitude vanish in the endpoints [6].

Momentum dependent constituent mass $M(p)$ preserves polynomiality, however it violates QCD Ward identities. The latter can be easily understood by the following example. Consider Dirac equation with a momentum dependent mass $M(p)$:

$$(\not{p} - M(p))\, u(p) = 0 \tag{1}$$

and the electromagnetic current

$$j^\mu = \overline{u}(p+q)\gamma^\mu u(p). \tag{2}$$

Naive current conservation reads

$$\begin{aligned} q_\mu j^\mu &= \overline{u}(p+q)\left[(\not{p}+\not{q}) - \not{p}\right] u(p) \\ &= [M(p+q) - M(p)]\, \overline{u}(p+q)u(p) \neq 0. \end{aligned} \tag{3}$$

Modifications of the electromagnetic current j^μ that make the current conserved have been proposed in Refs.[18] –[27]. The discussion of the low energy theorems in the context of the instanton model leading to the momentum dependent constituent quark mass with special emphasis on axial anomaly can be found in Ref.[28]. Although these modifications, supplied by an appropriate requirements of the absence of kinematical singularities [19] fix the longitudinal part of the pertinent non-local vertices, the transverse part remains undetermined. When one wishes to consider electromagnetic processes, it is necessary to assume some model for the transverse part. Therefore for the purpose of the present work we do not consider such modifications, although we acknowledge the fact that such a study is certainly required. Below we give an argument in favor of such a procedure that follows from the parametrical dependence of the current nonconservation in the instanton model of the QCD vacuum.

A non-local model leading to (1) can be "derived" from QCD in the instanton model of the QCD vacuum [29]. In this model the vacuum is filled with interacting instantons that stabilize in a configuration where the mean instanton radius $\rho \sim 1/(600 \text{ MeV})$, whereas the typical instaton separation $R \sim 1/(300 \text{ MeV})$. The instanton packing fraction $(\rho/R)^4$ is a dynamical small parameter of the model. The model allows to calculate $M(p)$ in Euclidean space. Setting $M(p) = MF^2(p)$ we have

$$F_{\text{inst.}}(p) = 2z\left[I_0(z)K_1(z) - I_1(z)K_0(z)\right] - 2I_1(z)K_1(z) \qquad (4)$$

where $z = p\rho/2$ and M is the constituent mass at zero momentum. Therefore (schematically)

$$\begin{aligned} M(p+q) - M(p) &= M\left[F^2((p+q)\rho) - F^2(p\rho)\right] \\ &\simeq M\frac{q\rho}{2}\frac{dF^2(z)}{dz}. \end{aligned} \qquad (5)$$

Equation (5) maybe viewed as an expansion in the inverse momentum $Q_{\text{inst.}} = 2/\rho$ corresponding to the typical instanton size. Hence for small momentum transfers (and this is certainly the domain of the present model) the nonconservation of the vector current is parametrically small in the inverse instanton size $Q_{\text{inst.}}$. Therefore in the following we shall use local currents, such as (2), rather than the non-local extensions, allowing for the violation of Ward identities at the level of $q/Q_{\text{inst.}}$. The price we pay for that is wrong normalization of the pertinent form factors, since it is fixed by the axial anomaly. However, the dependence on the kinematical variables is almost identical as in the models that preserve Ward identities. We shall come back to this point in Sect.6. Finally let us stress that despite the fact that our currents do not satisfy Ward identities the amplitudes we calculate

are gauge invariant, in the sense that they vanish when contracted with on-shell photon momentum.

3. Non-Local Chiral Quark Model

In order to provide non-local nonperturbative regulator we employ semi-bosonized Nambu–Jona-Lasinio model defined by the following action describing quark interaction with an external meson field U [29, 30]:

$$S_I = M \int \frac{d^4k d^4l}{(2\pi)^8} \bar{\psi}(k) F(k) U^{\gamma_5}(k-l) F(l) \psi(l) \qquad (6)$$

and $U^{\gamma_5}(x)$ can be expanded in terms of the pion fields:

$$U^{\gamma_5}(x) = 1 + \frac{i}{F_\pi} \gamma^5 \tau^A \pi^A(x) - \frac{1}{2F_\pi^2} \pi^A(x) \pi^A(x) + \dots \qquad (7)$$

M is a constituent quark mass of the order of 350 MeV and $F(k)$ is a momentum dependent function such that $F(0) = 1$ and $F(k^2 \to \infty) \to 0$. In what follows, for comparison, we will consider also $M = 225$ MeV

Note that (6) provides both momentum dependent mass of the quark fields and the non-local quark-meson coupling. Pions act at this stage only as auxiliary fields being – by equations of motion – objects composed from quark-antiquark fields. Kinetic term for pions appears only after integrating out the quark fields [30, 31] and the proper normalization is obtained by an appropriate choice of the cut-off function $F(k)$. Here, following Refs.[9, 6] we wish to perform all calculations in the Minkowski space. To this end we choose:

$$F(k) = \left(\frac{-\Lambda_n^2}{k^2 - \Lambda_n^2 + i\epsilon} \right)^n \qquad (8)$$

which reproduces reasonably well (4) for $k^2 < 0$. Numerical values of Λ_n for different choices of M are given in Table I of Ref.[6] and Table 1 of the present paper. Scale Λ_n should not be confused with the typical momentum scale Q_0 (which for the original shape of $F(k)$ given by Eq.(4) is equal to $Q_{\text{inst}} = 2/\rho$), that can be defined as the value of the momentum for which $F(Q_0) = \text{const.}$, say 1/2. Then

$$Q_0(n) = \Lambda_n \sqrt{\sqrt[n]{2} - 1} \qquad (9)$$

and does not exceed 2 GeV for the highest values of Λ_n.

Ansatz (8), apart from being close to the instanton motivated function (4), is very practical for calculations in the Minkowski space. Indeed, it

introduces a number of complex poles in the complex momentum plane, that can be analytically integrated over in the light cone coordinates. Light cone coordinates are defined by two null vectors: $\tilde{n} = (1,0,0,1)$ and $n = (1,0,0,-1)$. In this kinematical frame any four vector v can be decomposed as:

$$v^\mu = \frac{v^+}{2}\tilde{n}^\mu + \frac{v^-}{2}n^\mu + v_T^\mu \tag{10}$$

with $v^+ = n \cdot v$, $v^- = \tilde{n} \cdot v$ and the scalar product of two four vectors reads:

$$v \cdot w = \frac{1}{2}v^+w^- + \frac{1}{2}v^-w^+ - \vec{v}_T \cdot \vec{w}_T. \tag{11}$$

Therefore

$$k^2 - \Lambda_n^2 = k^-k^+ - \vec{k}_T^2 - \Lambda_n^2. \tag{12}$$

The integration measure in the light-cone coordinates takes the following form:

$$d^4k = dk^+ \, dk^- \, d^2\vec{k}_T/2. \tag{13}$$

Looking at (12) we see that (8) generates a n−th degree pole in the k^- plane that can be easily integrated over. The details can be found in Ref.[6] and in Sect.5.

4. Definitions and kinematics

We use the definitions of pion TDA's from [3] (our definitions include additional i phase factor)

$$\int \frac{d\lambda}{2\pi}e^{i\lambda Xp^+} \times \left\langle \gamma\left(P_2,\varepsilon\right)\left|\overline{d}\left(-\frac{\lambda}{2}n\right)\gamma^\mu u\left(\frac{\lambda}{2}n\right)\right|\pi^+\left(P_1\right)\right\rangle$$
$$= i\frac{ie}{2\sqrt{2}F_\pi p^+}\varepsilon^{\mu\nu\alpha\beta}\varepsilon_\nu^* p_\alpha q_\beta V\left(X,\xi,t\right) \tag{14}$$

$$\int \frac{d\lambda}{2\pi}e^{i\lambda Xp^+} \times \left\langle \gamma\left(P_2,\varepsilon\right)\left|\overline{d}\left(-\frac{\lambda}{2}n\right)\gamma^\mu\gamma_5 u\left(\frac{\lambda}{2}n\right)\right|\pi^+\left(P_1\right)\right\rangle$$
$$= i\frac{e}{2\sqrt{2}F_\pi p^+}P_2^\mu\left(q\cdot\varepsilon^*\right)A\left(X,\xi,t\right) + \dots \tag{15}$$

where $V\left(X,\xi,t\right)$ and $A\left(X,\xi,t\right)$ are vector and axial TDA respectively (we use $F_\pi = 93$ MeV). We shall use the following *symmetric* parametrization of momenta:

$$P_{1\mu} = \left(1+\xi\right)\frac{p^+}{2}\tilde{n}_\mu + \left(1-\xi\right)\frac{p^2}{2p^+}n_\mu - \frac{1}{2}q_\mu^T,$$
$$P_{2\mu} = \left(1-\xi\right)\frac{p^+}{2}\tilde{n}_\mu + \left(1+\xi\right)\frac{p^2}{2p^+}n_\mu + \frac{1}{2}q_\mu^T, \tag{16}$$

where $p_T = 0$, with

$$p_\mu = \frac{1}{2}(P_1 + P_2)_\mu = \frac{p^+}{2}\tilde{n}_\mu + \frac{p^2}{2p^+}n_\mu \qquad (17)$$

Here ξ denotes *skewedness*. Momentum transfer reads:

$$q_\mu = (P_2 - P_1)_\mu = -\xi p^+\tilde{n}_\mu + \xi\frac{p^2}{p^+}n_\mu + q_\mu^T. \qquad (18)$$

Note that q^2 is related to p^2. Indeed, using the on mass-shell condition (for $m_\pi = 0$):

$$0 = P_1^2 = P_2^2 = (1 - \xi^2)p^2 - \frac{1}{4}\vec{q}_T^2 = p^2 + \frac{1}{4}q^2$$

we arrive at:

$$4p^2 = -q^2 = -t > 0. \qquad (19)$$

Considering the momentum transfer squared:

$$q^2 = t = -4\xi^2 p^2 - \vec{q}_T^2, \quad \text{or} \quad -4\xi^2 p^2 = (t + \vec{q}_T^2), \qquad (20)$$

and inverting (20), we get an important constraint:

$$\vec{q}_T^2 = -(1 - \xi^2)t > 0 \qquad \rightarrow \qquad -1 < \xi < 1. \qquad (21)$$

One has to note, that the lower limit for ξ depends on the order of limits at $t = 0$ and $m_\pi \neq 0$ [4]. We have avoided this ambiguity by keeping $m_\pi = 0$ from the very beginning.

Photon polarization vector satisfies $\varepsilon^* \cdot P_2 = 0$. Dots in Eq.(15) stand for parts which are structure independent and thus irrelevant in our considerations [3, 4]. In general TDA's do not posses any symmetry properties in ξ and X - in contrary to GPD's [3].

One can define flavor diagonal VTDA's $V_u(X, \xi, t)$ and $V_d(X, \xi, t)$ by replacing in definition (14) π^+ by π^0 and taking operators $\overline{u}\left(-\frac{\lambda}{2}n\right)\gamma^\mu u\left(\frac{\lambda}{2}n\right)$ and $\overline{d}\left(-\frac{\lambda}{2}n\right)\gamma^\mu d\left(\frac{\lambda}{2}n\right)$ respectively. On the other hand matrix element $\langle\gamma(P_2, \varepsilon)|\overline{\psi}(0)\gamma^\mu\psi(0)|\pi^0(P_1)\rangle$, where ψ are now iso-doublets, is parameterized by the pion-photon transition form factor controlling $\gamma^*\gamma \to \pi^0$ processes. Therefore one can derive the sum rule [1] relating this form factor to $V_u(X, \xi, t)$ and $V_d(X, \xi, t)$. Its normalization is fixed by axial anomaly connected with the Ward identity relating matrix elements for transition of axial current to two photons with a similar matrix elements of a pseudoscalar current. This normalization together with the conventions of Eq.(14) gives the normalization condition for the VTDA:

$$\int\limits_{-1}^{1} dX\, V(X, \xi, t = 0) = \frac{N_c}{2\pi^2}(Q_u + Q_d) = \frac{1}{2\pi^2}, \qquad (22)$$

which is independent of M and of ξ. The latter is related to the polynomiality which states that the $n-$th moment of the TDA's in X is a polynomial in ξ of degree not higher than n. Normalization (22) is automatically satisfied in the local chiral quark model which in the chiral limit (*i.e.* for $m_\pi = 0$) gives the normalization of the ATDA of Eq.(15) equal to the one of the VTDA:

$$\int\limits_{-1}^{1} dX\, A\left(X, \xi, t = 0\right) = \frac{N_c}{6\pi^2}\left(Q_u - Q_d\right) = \frac{1}{2\pi^2}. \tag{23}$$

Note, however, that (23) is not fixed by the anomaly. This will be important in the non-local model where the two normalizations are not equal any more.

Moreover, we have the following sum rules relating vector and axial-vector form factors with the relevant TDA's

$$\int\limits_{-1}^{1} dX\, D\left(X, \xi, t\right) = \frac{2\sqrt{2}F_\pi}{m_\pi} F_D\left(t\right) = 2\sqrt{2}F_\pi F_D^\chi\left(t\right), \tag{24}$$

where D stands for V or A. In the chiral limit, which is considered in this paper, we define $F_V^\chi\left(t\right) = F_V\left(t\right)/m_\pi$ and similarly for F_A.

5. Transition distribution amplitudes in the chiral quark model

Using effective action (6) we obtain the following expressions for the matrix elements (14) and (15):

$$\int \frac{d\lambda}{2\pi} e^{i\lambda X p^+} \times \left\langle \gamma\left(P_2, \varepsilon\right) \left| \overline{d}\left(-\frac{\lambda}{2}n\right) \Gamma^\mu u\left(\frac{\lambda}{2}n\right) \right| \pi^+\left(P_1\right) \right\rangle$$

$$= -\frac{\sqrt{2}eMN_c}{F_\pi}\left(Q_d \mathcal{M}_1^{\mu\nu} + Q_u \mathcal{M}_2^{\mu\nu}\right)\varepsilon_\nu^*, \tag{25}$$

where Γ^μ is either γ^μ or $\gamma^\mu\gamma_5$, N_c is number of colors, Q_u and Q_d are charges of quarks u and d respectively. Two amplitudes $\mathcal{M}_1$ and $\mathcal{M}_2$ depicted in Fig.1 are defined as (we omit $i\epsilon$ prescription in fermion propagators):

$$\mathcal{M}_1^{\mu\nu} = \int \frac{d^4k}{(2\pi)^4}\, \delta\left(k^+ - (X-1)p^+\right) F\left(k\right) F\left(k+P_1\right) \times \tag{26}$$

$$\mathrm{Tr}\left\{\frac{1}{\not{k}+\not{P_2}-M\left(k+P_2\right)}\Gamma^\mu \frac{1}{\not{k}+\not{P_1}-M\left(k+P_1\right)}\gamma_5 \frac{1}{\not{k}-M\left(k\right)}\gamma^\nu\right\},$$

$$\mathcal{M}_2^{\mu\nu} = \int \frac{d^4k}{(2\pi)^4}\, \delta\left(k^+ - (X+1)p^+\right) F\left(k\right) F\left(k-P_1\right) \times \tag{27}$$

$$\mathrm{Tr}\left\{\frac{1}{\not{k}-\not{P_1}-M\left(k-P_1\right)}\Gamma^\mu \frac{1}{\not{k}-\not{P_2}-M\left(k-P_2\right)}\gamma^\nu \frac{1}{\not{k}-M\left(k\right)}\gamma_5\right\}.$$
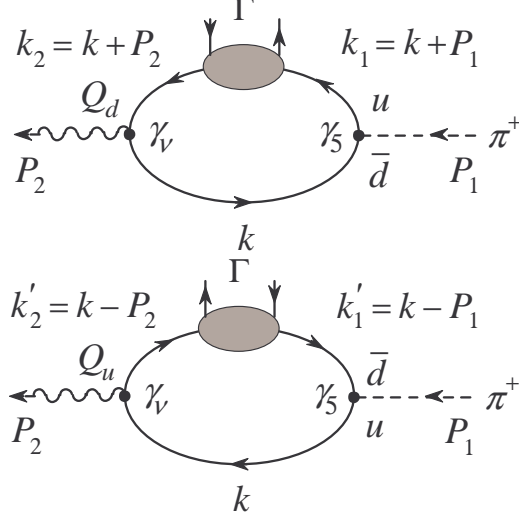
Fig. 1. Feynman diagrams for $\mathcal{M}_1$ and $\mathcal{M}_2$. Traces should be taken opposite to the momentum flow denoted by arrows. Time flows from right to left.

5.1. Local case

First we calculate TDA's neglecting the mass dependence upon p, *i.e.* we set $M(p) = M$. It was already done within a very similar model in Ref. [4], where the calculations were performed in the Minkowski space with Pauli-Villars regularization. In another approach partially discussed in Refs.[9]–[8] one uses the light cone coordinates (10) with the integration measure given by Eq.(13), performing first integration over dk^- and then over dk_T^2 with the transverse cut-off Λ^2. The latter is chosen to normalize appropriately F_π or alternatively to normalize the pion distribution amplitude to 1. Introducing transverse cut-off in the integrals defining TDA's would violate Lorentz invariance and, as a consequence, polynomiality. This can be nicely illustrated by considering the integral

$$I = \int \frac{d^4 k}{(2\pi)^4} \frac{1}{\left(k^2 - M^2\right)\left((k + P_2) - M^2\right)\left((k + P_1) - M^2\right)} \qquad (28)$$

which is related to the zeroth moment of the vector TDA and expanding it for small t:

$$I = \frac{-i}{8(2\pi)^2} \left\{ \int \frac{dk_T^2}{(k_T^2 + M^2)^2} + \frac{t}{4} \int dk_T^2 \frac{M^2}{(k_T^2 + M^2)^4} + \right.$$

$$\left. \frac{t}{12}\xi^2 \int dk_T^2 \frac{2k_T^2 - M^2}{(k_T^2 + M^2)^4} + \cdots \right\}. \tag{29}$$

Now, in order to make ξ^2 dependent term vanish

$$\int\limits_0^{\Lambda^2} dk_T^2 \frac{2k_T^2 - M^2}{(k_T^2 + M^2)^4} = -\frac{\Lambda^2}{(M^2 + \Lambda^2)^3} \tag{30}$$

we have to choose $\Lambda^2 = \infty$, what leads to:

$$I = \frac{-i}{8(2\pi)^2 M^2} \left\{ 1 + \frac{t}{12M^2} + \cdots \right\} \tag{31}$$

where ... denote higher powers of t.

So in order to preserve polynomiality we have to work with an infinite transverse cut-off. In this case it is very useful to switch to Euclidean space and use Schwinger representation for scalar propagators, following Ref.[5]. This allows to obtain analytical results in a very simple way. We shall be using TDA's calculated in the local model as a reference when discussing the results in the non-local case.

Calculating traces and combining definitions (14), (15) with (25) we get

$$V(X, \xi, t) = i16M^2 N_c p^+ \left(Q_d \mathcal{K}_1 + Q_u \mathcal{K}_2 \right), \tag{32}$$

$$A(X, \xi, t) = -\frac{i}{q \cdot \varepsilon^*} 16M^2 N_c p^+ \left(Q_d \mathcal{J}_1 + Q_u \mathcal{J}_2 \right), \tag{33}$$

where

$$\mathcal{K}_{1,2} = \int \frac{d^4k}{(2\pi)^4} \times \frac{\delta\left(k^+ - (X \mp 1)p^+\right)}{\left((k \pm P_1)^2 - M^2\right)\left((k \pm P_2)^2 - M^2\right)(k^2 - M^2)}, \tag{34}$$

$$\mathcal{J}_{1,2} = \int \frac{d^4k}{(2\pi)^4} \times \frac{\delta\left(k^+ - (X \mp 1)p^+\right)(\mp 2k + q) \cdot \varepsilon^*}{\left((k \pm P_1)^2 - M^2\right)\left((k \pm P_2)^2 - M^2\right)(k^2 - M^2)} \tag{35}$$

with upper signs referring to subscript "1" and lower signs to "2".

Taking the same steps as in [5], we get

$$
\begin{aligned}
\mathcal{K}_{1,2} \;=\; & \frac{-i}{(4\pi)^2\,p^+}\int_0^1 dy \int_0^{1-y} dz \\
& \times\; \delta\left(y\left(1+\xi\right)p^+ + z\left(1-\xi\right)p^+ \pm (X\mp 1)\right)\frac{1}{M^2 - yzt}, \quad (36)
\end{aligned}
$$

$$
\begin{aligned}
\mathcal{J}_{1,2} \;=\; & \frac{\pm iq\cdot\varepsilon^*}{(4\pi)^2\,P^+}\int_0^1 dy \int_0^{1-y} dz \\
& \times\; \delta\left(y\left(1+\xi\right)p^+ + z\left(1-\xi\right)p^+ \pm (X\mp 1)\right)\frac{1-2y}{M^2 - yzt}. \quad (37)
\end{aligned}
$$

While obtaining the second equation we used $n\cdot\varepsilon^* = 0$ (in the light-cone gauge), what made that expression finite. Let us notice that from these formulae it is obvious that TDA's satisfy polynomiality condition. Simple integration over Feynman parameters leads to the final result, which we quote in Appendix A.

The transition form factor we get in the local model recovers the normalization required by the axial anomaly. Its analytical form – calculated long time ago in Ref.[32] in more general kinematics – is given in Appendix B.

5.2. Non-local case

In this section we take full momentum dependence of the constituent quark mass in integrals (27) and (28). The calculations will be done in the Minkowski space. We use method of evaluating the contour integrals developed in Refs.[6, 8].

We start from VTDA. When evaluating the trace we find not only structures proportional to $\varepsilon^{\mu\nu\alpha\beta}\varepsilon^*_\nu p_\alpha q_\beta$, which are needed, but $\varepsilon^{\mu\nu\alpha\beta}\varepsilon^*_\nu n_\alpha P_{1\beta}$ and $\varepsilon^{\mu\nu\alpha\beta}\varepsilon^*_\nu n_\alpha P_{2\beta}$ as well. However they vanish when contracted with n_μ, thus they are unphysical in the sense that they do not give contribution to the observables. We obtain expressions of the following form

$$
\begin{aligned}
\mathcal{K}_{1,2} \;=\; & \int \frac{d^4 k}{(2\pi)^4}\,\frac{\delta\left(k^+ - (X\mp 1)\,p^+\right)F(k)\,F(k\pm P_1)}{D(k\pm P_1)\,D(k\pm P_2)\,D(k)} \\
& \times\; \frac{1}{M}\left\{A_{1,2}\,M(k\pm P_1) + B_{1,2}\,M(k\pm P_2) + C_{1,2}\,M(k)\right\} \quad (38)
\end{aligned}
$$

where

$$
D(p) = p^2 - M^2(p) + i\epsilon. \quad (39)
$$

Fuctions $A_{1,2}$, $B_{1,2}$, $C_{1,2}$ depend on X, ξ, t and integration variable $\vec{k}_T$. Their explicit form is given in Appendix C.

Next, we have to take mass dependence on momentum given by (8). We choose Λ_n for given n in such a way that pion DA calculated in the present model is normalized to unity. Pertinent values of Λ_n are listed in Table 1.

n	1	2	3	5
$M = 350\,\mathrm{MeV}$	1156	1727	2155	2819
$M = 225\,\mathrm{MeV}$	2121	3125	3880	5060

Table 1. Values (in MeV) of Λ in function of n for $M = 350$ and 225 MeV.

Introducing dimensionless variables $\kappa = k/\Lambda$, $\bar{P}_1 = P_1/\Lambda$, $\bar{P}_2 = P_2/\Lambda$, $r = M/\Lambda$ and using

$$u_{1,2}^{\pm} = \left(\kappa \pm \bar{P}_{1,2}\right)^2 - 1 + i\epsilon, \tag{40}$$

$$u_3 = \kappa^2 - 1 + i\epsilon, \tag{41}$$

we get

$$
\begin{aligned}
\mathcal{K}_{1,2} = \frac{1}{2M\Lambda^3} \int \frac{d^2\kappa_T dk^- d\kappa^+}{(2\pi)^4} \quad & \frac{\delta\left(\kappa^+ - (X \mp 1)\,\bar{p}^+\right)}{G\left(u_1^{\pm}\right) G\left(u_2^{\pm}\right) G(u_3)} \\
\times & \left\{ A_{1,2} \left(u_1^{\pm}\right)^n \left(u_2^{\pm}\right)^{4n} \left(u_3^{\pm}\right)^{3n} \right. \\
& +B_{1,2} \left(u_1^{\pm}\right)^{3n} \left(u_2^{\pm}\right)^{2n} \left(u_3^{\pm}\right)^{3n} \\
& \left. +C_{1,2} \left(u_1^{\pm}\right)^{3n} \left(u_2^{\pm}\right)^{4n} \left(u_3^{\pm}\right)^{n} \right\}, \quad (42)
\end{aligned}
$$

where $G(u) = u^{4n+1} + u^{4n} - r^2$. Polynomial $G(u)$ can be alternatively written in a factorized form $G(u) = \prod_{i=1}^{4n+1}(u - z_i)$, where z_i are roots of equation $G(u) = 0$ and can be found numerically. Note, that if $r = 0$ (*i.e.* $\Lambda \to \infty$) we have $4n$ degenerate solutions equal to zero and one equal to -1. If Λ becomes finite the degeneracy is lifted and we have $4n + 1$ solutions which in general are complex. Integration over $d\kappa^-$ has to be done by the residue theorem, thus we have to find the poles in κ^- complex plane. However, because of the imaginary part of $z_i{'}$s, the poles can cross the standard integration contour. This may result in non-vanishing of the TDA's in unphysical regions. To avoid this, the integration contour has to be modified. Detailed discussion of these problems is given in [6] and

Appendix C. After performing the contour integrals we get:

$$
\mathcal{K}_{1,2} \;=\; \frac{i}{2\Lambda^3 \bar{p}^+} \sum_{i,j,k=1}^{4n+1} f_i f_j f_k \int \frac{d^2\kappa_T}{(2\pi)^3} \tag{43}
$$

$$
\frac{A_{1,2} z_i^{p_{1,2}} z_j^{r_{1,2}} z_k^{s_{1,2}} + B_{1,2} z_i^{a_{1,2}} z_j^{b_{1,2}} z_k^{c_{1,2}} + C_{1,2} z_i^{d_{1,2}} z_j^{e_{1,2}} z_k^{g_{1,2}}}{(\alpha_{1,2} z_i - z_j + \beta_{1,2})(\gamma_{1,2} z_i - z_k + \rho_{1,2})},
$$

where

$$
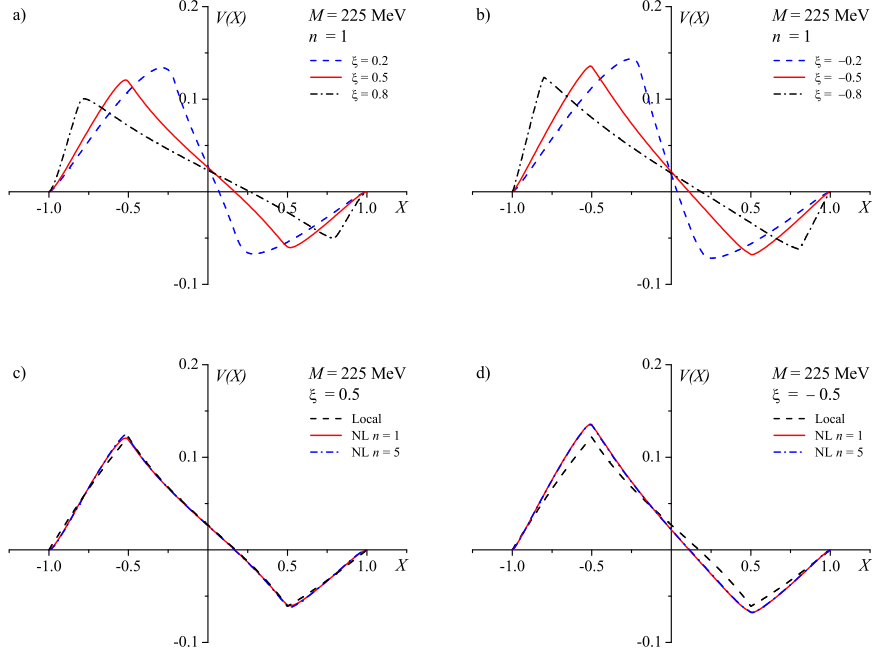f_i = \prod_{j\neq i}^{4n+1} (z_i - z_j)^{-1} \tag{44}
$$
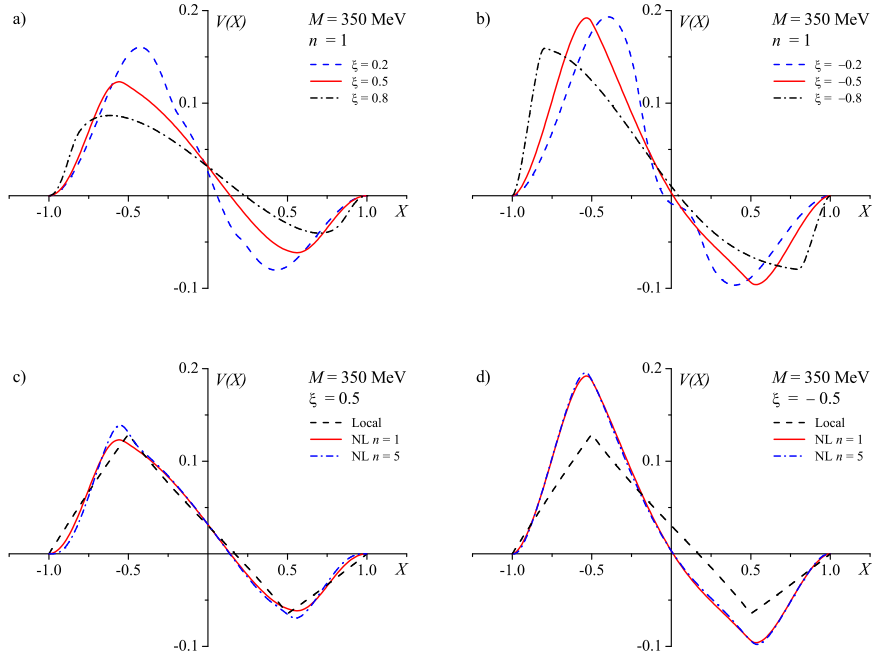
Fig. 2. Vector TDA's in the non-local model: a) for $n = 1$ and $\xi = 0.2$ (dashed), $\xi = 0.5$ (solid), $\xi = 0.8$ (dash-dot); b) for $n = 1$ and $\xi = -0.2$ (dashed), $\xi = -0.5$ (solid), $\xi = -0.8$ (dash-dot). Comparison of the local model: c) for $\xi = 0.5$ (dashed) with the non-local model for $n = 1$ (solid) and $n = 5$ (dash-dot); d) for $\xi = -0.5$ (dashed) with the non-local model for $n = 1$ (solid) and $n = 5$ (dash-dot). All plots are made for constituent quark mass $M = 350\,\mathrm{MeV}$ and $t = -0.1\,\mathrm{GeV}^2$.

Fig. 3. Vector TDA's in the non-local model: a) for $n = 1$ and $\xi = 0.2$ (dashed), $\xi = 0.5$ (solid), $\xi = 0.8$ (dash-dot); b) for $n = 1$ and $\xi = -0.2$ (dashed), $\xi = -0.5$ (solid), $\xi = -0.8$ (dash-dot). Comparison of the local model: c) for $\xi = 0.5$ (dashed) with the non-local model for $n = 1$ (solid) and $n = 5$ (dash-dot); d) for $\xi = -0.5$ (dashed) with the non-local model for $n = 1$ (solid) and $n = 5$ (dash-dot). All plots are made for constituent quark mass $M = 225 \, \text{MeV}$ and $t = -0.1 \, \text{GeV}^2$.

Here powers of z_i-s (denoted by Latin characters), as well as the explicit form of the functions $\alpha_{1,2}$, $\beta_{1,2}$, $\gamma_{1,2}$, $\rho_{1,2}$ depend on the region of X (see Appendix C). It should be pointed out that expressions denoted by Greek characters contain second power of κ_T, while functions $A_{1,2}$, $B_{1,2}$, $C_{1,2}$ are of first order in κ_T. Therefore the integration over $d^2\kappa_T = \kappa_T d\kappa_T d\theta_T$ is finite. Integral over $d\theta_T$ can be done analytically by integration over a unit circle, while integral $d\kappa_T$ can be performed numerically.

In the non-local model we cannot recover the required normalization (22) for finite Λ. This can be understood as a consequence of the regularization that does not respect axial anomaly. Therefore we impose the proper normalization (22) by multiplying the VTDA by a suitable correction factor N_V as given in Table 2.

Results for VTDA are shown in Figs.2 and 3 for constituent masses $M = 350$ and 225 MeV respectively. We observe that the "non-local" curves are less sharp than in the local case and that their shape depends slightly on n. Also the maxima are shifted from $X = \pm\xi$, where they were placed in local case. The non-local model has the feature that VTDA's are no more ξ-symmetric and for $\xi < 0$ it gives results that are more peaked than in the local case and with the middle zero in a different position. The deviation from the local model is stronger for larger constituent masses.
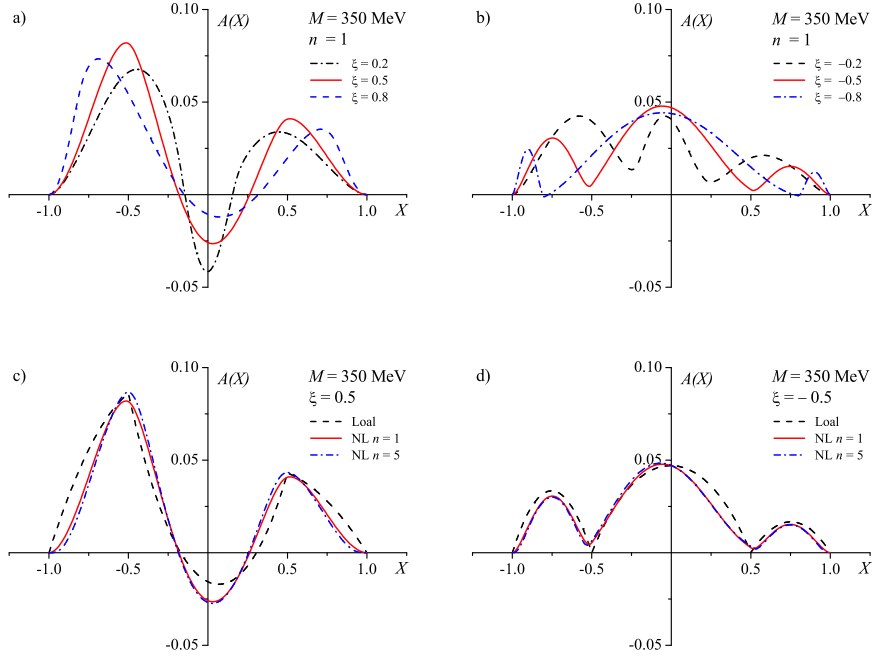

Fig. 4. Axial TDA's in the non-local model: a) for $n = 1$ and $\xi = 0.2$ (dashed), $\xi = 0.5$ (solid), $\xi = 0.8$ (dash-dot); b) for $n = 1$ and $\xi = -0.2$ (dashed), $\xi = -0.5$ (solid), $\xi = -0.8$ (dash-dot). Comparison of the local model: c) for $\xi = 0.5$ (dashed) with the non-local model for $n = 1$ (solid) and $n = 5$ (dash-dot); d) for $\xi = -0.5$ (dashed) with the non-local model for $n = 1$ (solid) and $n = 5$ (dash-dot). All plots are made for constituent quark mass $M = 350\,\text{MeV}$ and $t = -0.1\,\text{GeV}^2$.

In the case of axial TDA's the algebraical steps are the same. The complication is that after evaluating the trace we have to retain only terms proportional to $P_2^\mu (q \cdot \varepsilon^*)$, since all other terms are structure independent or gauge artifacts. General expression is similar to (44), but now functions

A, B, C contain also second power of κ_T. However, the integration over $d\kappa_T$ is finite because of the property:

$$\sum_{i=1}^{4n+1} z_i^m f_i = \begin{cases} 0 & \text{if} \quad m < 4n \\ 1 & \text{if} \quad m = 4n \end{cases} \tag{45}$$
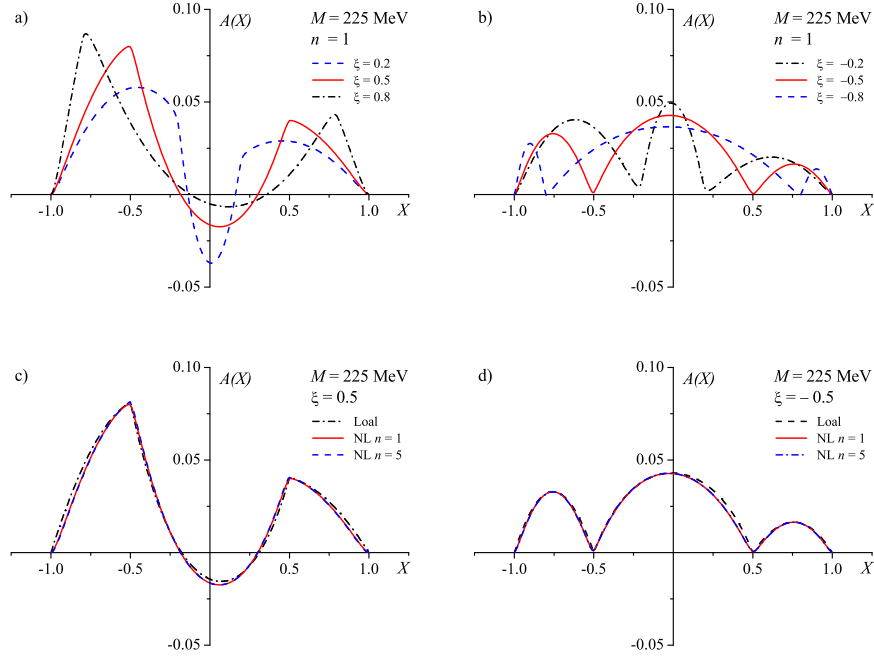
(see again [6] and Appendix C).

Fig. 5. Axial TDA's in the non-local model: a) for $n = 1$ and $\xi = 0.2$ (dashed), $\xi = 0.5$ (solid), $\xi = 0.8$ (dash-dot); b) for $n = 1$ and $\xi = -0.2$ (dash-dot), $\xi = -0.5$ (solid), $\xi = -0.8$ (dashed). Comparison of the local model: c) for $\xi = 0.5$ (dashed) with the non-local model for $n = 1$ (solid) and $n = 5$ (dash-dot); d) for $\xi = -0.5$ (dashed) with the non-local model for $n = 1$ (solid) and $n = 5$ (dash-dot). All plots are made for constituent quark mass $M = 225\,\text{MeV}$ and $t = -0.1\,\text{GeV}^2$.

Numerical results for the ATDA's are shown in Figs.4 and 5 for constituent masses $M = 350$ and 225 MeV respectively. W see again that to a good accuracy all models (local and fully non-local one for different n) give the same results both for positive and for negative ξ (note, however, small shift of the minima in the non-local case). All curves were normalized as in

the local case according to Eq.(23), multiplying the calculated distribution by correction factors listed in Table 3. Again the deviation from the local model is stronger for larger constituent masses.

We have checked numerically that TDA's in the non-local model satisfy polynomiality condition for first three moments. However, contrary to the local case, even moments of VTDA are nonzero.

6. Summary and discussion

In the present paper we have employed chiral quark model with momentum dependent constituent quark mass to calculate pion-to-photon transition distribution amplitudes. Before we briefly summarize our results let us discuss the main features of the model. We have chosen momentum dependence in the simple form given in Eq.(8) which for Euclidean momenta resembles $M(p)$ obtained within the instanton model of the QCD vacuum. This form of $M(p)$ allows to perform all integrations directly in the Minkowski space and has been previously applied to calculate pion [6] and kaon [25] distribution amplitudes and two pion distributions as well as generalized parton distribution of the pion [8]. The main technicality that we wish to mention, consists in the proper choice of the integration contour in the loop momentum k^- which is discussed in Appendix C and can be also found in Ref.[6].

Proper choice of the integration contour guaranties that the TDA's are real and have proper support in kinematical variables X and ξ defined in Sect.4 and satisfy polynomiality.

Throughout this paper we have used momentum dependent mass that acts as an UV cutoff and, at the same time, as the quark form factor within the pion. The latter is very important for making the pion DA vanish in the endpoints [6, 9]. Indeed, similar calculation of the photon DA yields distribution that is discontinuous in the endpoints [10] reflecting the point-like nature of the quark-photon coupling.

Although we have used momentum dependent mass, we have not modified currents accordingly [18]–[27], and as a consequence our model violates QCD Ward identities. This violation is however "mild" as it occurs at the level $q\rho/2$ where ρ is the mean instanton radius (5). Nevertheless violation of the axial Ward identity results in the wrong normalization of the vector TDA which is fixed by the axial anomaly. In order to get over this deficiency we have simply corrected normalization of VTDA to the value obtained in the local model which does satisfy axial Ward identity. The correction factors (model results should be multiplied by N_V or N_A to obtain normalization of Eqs.(22,23)) are given in Tables 2 and 3 and may seem large. Local limit can be obtained by pushing artificially $\Lambda \to \infty$ in (8).

Obviously the same procedure applied to the pion DA would yield pion DA
constant, but with an infinite norm. In that case correction factor would be
infinite (modulo some regularization such as a transverse cutoff for exam-
ple). On this scale correction factors of the order of 1.5 are not excessively
large.

M	$n = 1$	$n = 2$	$n = 3$	$n = 5$
225 MeV	1.151	1.148	1.147	1.146
350 MeV	1.487	1.490	1.490	1.491

Table 2. Correction factors N_V for VTDA for $M = 225$ and 350 MeV and different
values of n.

M	$n = 1$	$n = 2$	$n = 3$	$n = 5$
225 MeV	1.083	1.081	1.081	1.080
350 MeV	1.217	1.219	1.219	1.219

Table 3. Correction factors N_A for ATDA for $M = 225$ and 350 MeV and different
values of n

Despite the fact that Ward identities are not satisfied our amplitudes are
gauge invariant, *i.e.* they vanish when contracted with photon momentum.

Normalization of axial TDA's is not fixed by the anomaly. However, in
order to compare them with local model we used correction factors fixing
normalization given by (23). This normalization overshoots experiment by
approximately a factor of 2. Such a large mismatch is common to local
quark models [5]. The correction procedure used in this paper to maintain
normalizations (22) and (23) is to large extent arbitrary. Taking normal-
izations as they come out (*i.e.* without correction factors $N_{V,A}$) would shift
the axial transition form factor at $t = 0$ towards the experimental value.
At the same time VTDA would loose correct normalization. The latter,
however, should be attributed to the violation of the Ward identities in
the present version of the model and it is the violation of the axial anomaly
which is responsible for the wrong normalization in the vector case. Clearly,
only a complete calculation with the non-local currents might resolve this
discrepancy.

Transition form factors are defined in Eq.(24). We show them in Fig.6.
All calculations were performed for the constituent quark mass $M = 350$
and $M = 225$ MeV. We find that in the case of the non-local model the
transition form factor is more dumped than the one calculated in the local
version. However, for realistic constituent quark mass $M = 350$ MeV it
still falls off much slower than the experimental curve parameterized by the

function [33]

$$F_{\pi\gamma}^{exp}(t) = \frac{F_{\pi\gamma}(0)}{1 - t/M_0^2}, \qquad (46)$$

where $M_0 = 776\,\mathrm{MeV}$. We could get good description of experimental data for much lower values of constituent quark mass parameter M. This can be easily understood from the approximate formula (31) where the slope reads

$$M_0^2 = 12M^2 \rightarrow M = 225 \text{ MeV}.$$

For that reason we have used $M = 225$ MeV for our calculations although the reasonable values of the constituent masses that have been used in in the literature – as explained in Sect. 1 – lie above 300 MeV.
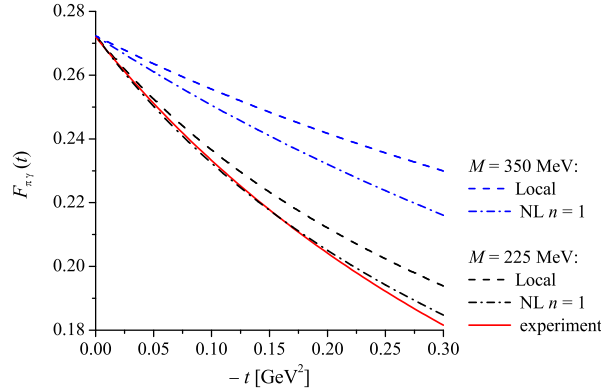

Fig. 6. Comparison of the transition form factors obtained in various versions of the chiral quark model. Solid line represents experimental fit of Eq.(46). Dashed lines correspond to local model, dash-dotted lines to the non-local one with $n = 1$ (there is almost no n dependence). Two upper curves correspond to $M = 350$ MeV, two lower ones to $M = 225$ MeV.

Our calculations were performed in the symmetric kinematics defined in Sect.4 and can be directly compared with Ref.[4]. There is qualitative agreement between the local version of the present model and the one of Ref.[4] (up to an overall sign of ξ for the axial case, see Ref.[34]). In order to make comparison with [5] we have repeated their calculations in our kinematics. The results are essentially identical to the local version of the present model, provided we take small constituent mass. This is illustrated in Figs. 7 where we plot vector and axial TDA's for $\xi = \pm 0.5$ and $t = -0.3$

GeV^2 in SQM and local version of the present model for $M = 225$ and 350 MeV.
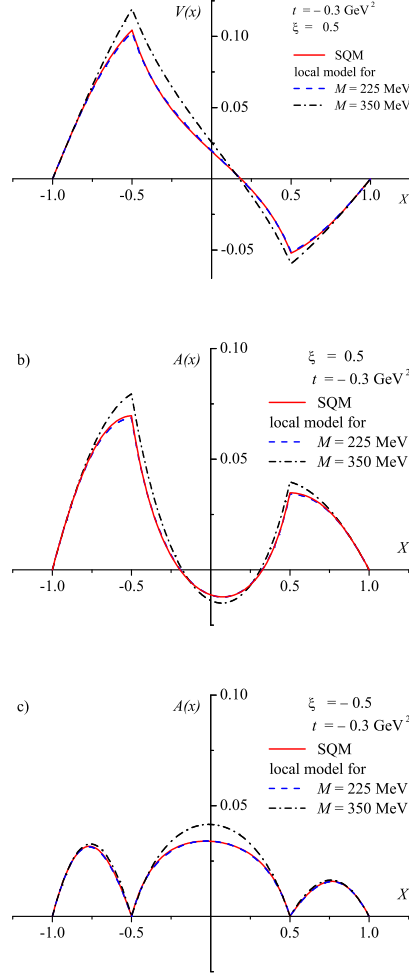

Fig. 7. Comparison of vector (a) and axial (b,c) TDA's obtained in the SQM of Ref. [5] (solid) with the local version of the present model for $M = 225$ MeV (dashed), $M = 350$ MeV (dash-dot) and $\xi = \pm 0.5$ (a), 0.5 (b) and -0.5 (c). Plots are made for $t = -0.3$ MeV.

We see that the pion-to-photon transition amplitudes defined in Eqs.(14) and (15) are quite robust. Basically their shapes do not depend on the specific model and on the regularization used. Nevertheless some small

differences between local and non-local models can be observed. The most prominent is the violation of the $\xi-$symmetry present in the local case for the vector TDA which can be seen in Figs.2 and 3. For negative ξ the non-local model gives results that are more peaked than in the local case and with the middle zero in a different position. On the other hand ATDA's are very close to the local case. One may be therefore confident that the shape of the axial TDA is without doubts as shown in Figs.4 and 5, however normalization is not certain and should be perhaps adjusted to the experimental value of the axial transition form factor.

From the point of view of QCD the quantities we calculate depend on a nonperturbative scale Q_0 which, however, must not be confused neither with the constituent mass M nor with an auxiliary parameter Λ. For $k^2 < 0$ the Ansatz (8) should imitate $M(k)$ obtained from the instantons. And for the latter, as explained in the Introduction, $Q_0 \sim 2/\rho = 1200$ MeV. It is therefore natural to assume that Q_0 is of the order of 1 GeV irrespectively of M and Λ. The precise definition of Q_0 is only possible within QCD and in all effective models one can use only qualitative *order of magnitude* arguments to estimate Q_0. Discussion of this point can be found in Ref.[6]. Once the nonperturbative scale Q_0 is fixed, our results should be evolved to the hard scale characterizing given experimental setup by means of the evolution equations discussed recently at length in Ref. [35]. This will be a subject of a separate study.

Acknowledgements

Appendix A

Transition distribution amplitudes in the local model

According to notation introduced in Sect. 5.1 we obtained the following expressions for VTDA (we quote results for positive ξ, due to the $\xi - $ symmetry)

$$
\mathcal{K}_{1,2} = \frac{-i}{(4\pi)^2 \, p^+} \Bigg\{ \theta\left(X+\xi\right) \theta\left(\xi - X\right) \frac{\mathrm{sign}\left(a_{1,2} - C_{1,2}\right)}{2\sqrt{AB_{1,2}}}
$$
$$
\ln \left| \frac{(a_{1,2} - C_{1,2})(b_{1,2} + C_{1,2})}{(a_{1,2} + C_{1,2})(b_{1,2} - C_{1,2})} \right|
$$
$$
+ \theta\left(1 \mp X\right) \theta\left(\pm X - \xi\right) \frac{\mathrm{sign}\left(a_{1,2} - C_{1,2}\right)}{\sqrt{AB_{1,2}}} \ln\left| \frac{a_{1,2} - C_{1,2}}{a_{1,2} + C_{1,2}} \right| \Bigg\} \quad \text{(A.1)}
$$

where $A = (1+\xi)\,t$, $C_{1,2} = \sqrt{B_{1,2}/A}$ and

$$
a_{1,2} = \frac{1 \mp X}{2\left(1 + \xi\right)} \tag{A.2}
$$

$$
b_{1,2} = \frac{\xi^2 \mp X}{2\xi\left(1 + \xi\right)} \tag{A.3}
$$

$$
B_{1,2} = \frac{(X \mp 1)^2 \, t^2}{4A} - (1 - \xi) M^2 . \tag{A.4}
$$

We remind that upper signs refer to subscript "1". For ATDA we have for positive ξ

$$
\mathcal{J}_{1,2}\left(\xi > 0\right) = \frac{\pm iq \cdot \varepsilon}{(4\pi)^2 \, p^+} \Bigg\{ \theta\left(X+\xi\right) \theta\left(\xi - X\right) \frac{\left(1 + D_{1,2}\right) \mathrm{sign}\left(a_{1,2} - C_{1,2}\right)}{2\sqrt{AB_{1,2}}}
$$
$$
\times \left(\ln\left| \frac{(a_{1,2} - C_{1,2})(b_{1,2} + C_{1,2})}{(a_{1,2} + C_{1,2})(b_{1,2} - C_{1,2})} \right| - \frac{1}{A} \ln\left| \frac{Aa_{1,2}^2 - B_{1,2}}{Ab_{1,2}^2 - B_{1,2}} \right| \right)
$$
$$
+ \theta\left(1 \mp X\right) \theta\left(\mp X - \xi\right) \frac{\left(1 + D_{1,2}\right) \mathrm{sign}\left(a_{1,2} - C_{1,2}\right)}{\sqrt{AB_{1,2}}} \ln\left| \frac{a_{1,2} - C_{1,2}}{a_{1,2} + C_{1,2}} \right| \Bigg\}
$$
$$
\tag{A.5}
$$

and for negative ξ

$$
\begin{aligned}
\mathcal{J}_{1,2}\left(\xi<0\right) = \frac{\pm iq\cdot\varepsilon}{\left(4\pi\right)^2 p^+} & \left\{ \theta\left(X-\xi\right)\theta\left(-\xi-X\right)\frac{\left(1+D_{1,2}\right)\mathrm{sign}\left(a_{1,2}-C_{1,2}\right)}{2\sqrt{AB_{1,2}}} \right. \\
& \times \left(\ln\left|\frac{\left(a_{1,2}-C_{1,2}\right)\left(b_{1,2}-C_{1,2}\right)}{\left(a_{1,2}+C_{1,2}\right)\left(b_{1,2}+C_{1,2}\right)}\right| - \frac{1}{A}\ln\left|\frac{Aa_{1,2}^2-B_{1,2}}{Ab_{1,2}^2-B_{1,2}}\right| \right) \\
+ \theta\left(1\mp X\right)\theta\left(\pm X\mp\xi\right) & \left. \frac{\left(1+D_1\right)\mathrm{sign}\left(a_1-C_1\right)}{\sqrt{AB_1}}\ln\left|\frac{a_{1,2}-C_{1,2}}{a_{1,2}+C_{1,2}}\right| \right\} \quad \text{(A.6)}
\end{aligned}
$$

We introduced above

$$
D_1 = \frac{X-1}{1+\xi} \qquad D_2 = -\frac{X+1}{1+\xi}. \tag{A.7}
$$

All the remaining notation is the same as in the VTDA case.

Appendix B

Transition form factor in the local model

We obtain the following expression for the pion-photon transition form factor

$$
F_{\pi\gamma}\left(t\right) = \frac{M^2}{2\pi^2 F_\pi}\frac{1}{t}\left[\mathrm{Li}_2\left(\frac{1}{\alpha_+}\right)+\mathrm{Li}_2\left(\frac{1}{\alpha_-}\right)\right], \tag{B.1}
$$

where

$$
\alpha_\pm = \frac{1}{2}\left(1\pm\sqrt{1-\frac{4M^2}{t}}\right) \tag{B.2}
$$

and $\mathrm{Li}_2\left(x\right)$ is the dilogarithm function, defined as $\mathrm{Li}_2\left(x\right) = -\int_0^x \frac{\ln(1-t)}{t}\, dt$.

Appendix C

TDA's in non-local model

In Fig.8 integration contour on the κ^- complex plane is schematically shown. As explained in more detail in main text, contour is chosen in such a way that poles form each group cannot cross it.
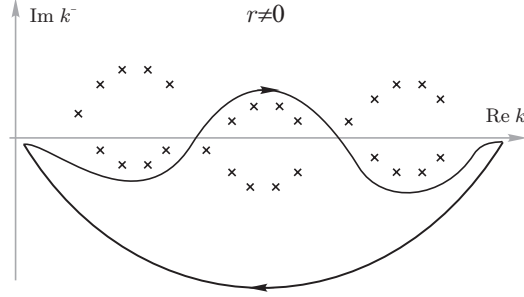
Fig. 8. Integration contour on the κ^- complex plane for $r = M/\Lambda \neq 0$. When $r \to 0$ the poles from each group merge into one pole and contour becomes standard semicircle.

In the case of VTDA we have the following general formula for the integrals (38)

$$
\mathcal{K}_{1,2} = \frac{i}{2\Lambda^3 \bar{p}^+} \sum_{i,j,k=1}^{4n+1} f_i f_j f_k \int \frac{d^2 \kappa_T}{(2\pi)^3} \epsilon_{1,2}
$$

$$
\frac{A_{1,2} z_i^{p_{1,2}} z_j^{r_{1,2}} z_k^{s_{1,2}} + B_{1,2} z_i^{a_{1,2}} z_j^{b_{1,2}} z_k^{c_{1,2}} + C_{1,2} z_i^{d_{1,2}} z_j^{e_{1,2}} z_k^{g_{1,2}}}{(\alpha_{1,2} z_i - z_j + \beta_{1,2})(\gamma_{1,2} z_i - z_k + \rho_{1,2})}. \quad \text{(C.1)}
$$

First consider $\xi > 0$ case. For $A_{1,2}$, $B_{1,2}$, $C_{1,2}$ we have the following expressions:

$$
A_{1,2} = \mp \frac{1}{2}(X \mp 1) \mp \frac{\Lambda^2 \vec{\kappa}_T \cdot \vec{q}_T}{(1+\xi)\, t} \quad \text{(C.2)}
$$

$$
B_{1,2} = \pm \frac{1}{2}(X \mp 1) \mp \frac{\Lambda^2 \vec{\kappa}_T \cdot \vec{q}_T}{(1-\xi)\, t} \quad \text{(C.3)}
$$

$$
C_{1,2} = 1 \pm \frac{2\Lambda^2 \vec{\kappa}_T \cdot \vec{q}_T}{(1-\xi^2)\, t}. \quad \text{(C.4)}
$$

The explicit form of $\alpha_{1,2}$, $\beta_{1,2}$, $\gamma_{1,2}$, $\rho_{1,2}$ and $\epsilon_{1,2}$ depends on the region of the support under consideration. We introduce

$$
u_a^{1,2} = \pm \frac{(X \mp 1)(1-\xi)\, t}{4\Lambda^2 \bar{p}^+ (X \pm \xi)} + \frac{\kappa_T^2 \mp \vec{\kappa}_T \cdot \vec{q}_T + 1}{\bar{p}^+ (X \pm \xi)} \quad \text{(C.5)}
$$

$$
u_b^{1,2} = \pm \frac{(X \mp 1)(1+\xi)\, t}{4\Lambda^2 \bar{p}^+ (X \mp \xi)} + \frac{\kappa_T^2 \pm \vec{\kappa}_T \cdot \vec{q}_T + 1}{\bar{p}^+ (X \mp \xi)} \quad \text{(C.6)}
$$

$$u_c^{1,2} = \frac{\kappa_T^2 + 1}{\bar{p}^+ \left(X \mp 1\right)}. \tag{C.7}$$

In every region we have:

- $-1 \leq X < -\xi$

$$\epsilon_1 = 0, \quad \epsilon_2 = -\frac{1}{X + 1} \tag{C.8}$$

$$\alpha_2 = \frac{X + \xi}{X + 1}, \quad \gamma_2 = \frac{X - \xi}{X + 1} \tag{C.9}$$

$$\beta_2 = \bar{p}^+ \left(X + \xi\right) \left(u_c^2 - u_b^2\right) \tag{C.10}$$

$$\rho_2 = \bar{p}^+ \left(X - \xi\right) \left(u_c^2 - u_a^2\right) \tag{C.11}$$

- $-\xi \leq X < \xi$

$$\epsilon_{1,2} = \mp \frac{1}{X \pm \xi} \tag{C.12}$$

$$\alpha_{1,2} = \frac{X \mp \xi}{X \pm \xi}, \quad \gamma_{1,2} = \frac{X \mp 1}{X \pm \xi} \tag{C.13}$$

$$\beta_{1,2} = \bar{p}^+ \left(X \mp \xi\right) \left(u_a^{1,2} - u_b^{1,2}\right) \tag{C.14}$$

$$\rho_{1,2} = \bar{p}^+ \left(X \mp 1\right) \left(u_a^{1,2} - u_c^{1,2}\right) \tag{C.15}$$

- $\xi \leq X \leq 1$

$$\epsilon_1 = \frac{1}{X - 1}, \quad \epsilon_2 = 0 \tag{C.16}$$

$$\alpha_1 = \frac{X - \xi}{X - 1}, \quad \gamma_1 = \frac{X + \xi}{X - 1} \tag{C.17}$$

$$\beta_1 = \bar{p}^+ \left(X - \xi\right) \left(u_c^1 - u_b^1\right) \tag{C.18}$$

$$\rho_1 = \bar{p}^+ \left(X + \xi\right) \left(u_c^1 - u_a^1\right) \tag{C.19}$$

Powers of z_i-s in the numerator can also be different in each interval. They read

- $-1 \leq X < -\xi$ and $\xi \leq X \leq 1$

$$p_{1,2} = 3n, \qquad r_{1,2} = 4n, \qquad s_{1,2} = n \qquad \text{(C.20)}$$

$$a_{1,2} = 3n, \qquad b_{1,2} = 2n, \qquad c_{1,2} = 3n \qquad \text{(C.21)}$$

$$d_{1,2} = n, \qquad e_{1,2} = 4n, \qquad g_{1,2} = 3n \qquad \text{(C.22)}$$

- $-\xi \leq X < \xi$

$$p_1 = n, \qquad r_1 = 3n, \qquad s_1 = 4n \qquad \text{(C.23)}$$

$$a_1 = 3n, \qquad b_1 = 2n, \qquad c_1 = 3n \qquad \text{(C.24)}$$

$$d_1 = 3n, \qquad e_1 = n, \qquad g_1 = 4n \qquad \text{(C.25)}$$

$$p_2 = n, \qquad r_2 = 4n, \qquad s_2 = 3n \qquad \text{(C.26)}$$

$$a_2 = 3n, \qquad b_2 = 2n, \qquad c_2 = 3n \qquad \text{(C.27)}$$

$$d_2 = 3n, \qquad e_2 = 4n, \qquad g_2 = n \qquad \text{(C.28)}$$

For negative ξ we have to change from Eqs. (C.8-C.19) only Eqs. (C.12-C.15). Appropriate expressions read

$$\epsilon_{1,2} = \mp \frac{1}{X \mp \xi} \qquad \text{(C.29)}$$

$$\alpha_{1,2} = \frac{X \pm \xi}{X \mp \xi}, \quad \gamma_{1,2} = \frac{X \mp 1}{X \mp \xi} \qquad \text{(C.30)}$$

$$\beta_{1,2} = \bar{p}^+ (X \pm \xi) \left(u_b^{1,2} - u_a^{1,2} \right) \qquad \text{(C.31)}$$

$$\rho_{1,2} = \bar{p}^+ (X \mp 1) \left(u_b^{1,2} - u_c^{1,2} \right). \qquad \text{(C.32)}$$

Also Eqs. (C.23-C.28) have to be replaced by

$$p_{1,2} = 4n, \qquad r_{1,2} = n, \qquad s_{1,2} = 3n \qquad \text{(C.33)}$$

$$a_{1,2} = 2n, \qquad b_{1,2} = 3n, \qquad c_{1,2} = 3n \qquad \text{(C.34)}$$

$$d_{1,2} = 4n, \qquad e_{1,2} = 3n, \qquad g_{1,2} = n \qquad \text{(C.35)}$$

In the case of ATDA the general formula for $\mathcal{J}_{1,2}$ is the same as for VTDA, but now we have different expressions for $A_{1,2}$, $B_{1,2}$, $C_{1,2}$. They are

$$A_{1,2} = g^{\mp} \pm 2v^{\mp} \qquad \text{(C.36)}$$

$$B_{1,2} = -f^{\mp} - g^{\mp} \tag{C.37}$$

$$C_{1,2} = -2g^{\mp} \mp 2v^{\mp} + f^{\mp} \pm 1, \tag{C.38}$$

where

$$f^{\pm} = \pm 1 + X - \frac{2\xi\Lambda^2 \vec{\kappa}_T \cdot \vec{q}_T}{(1-\xi^2)\,t} \tag{C.39}$$

$$g^{\pm} = -\frac{1}{2}(X \pm 1) - \frac{\Lambda^2 \vec{\kappa}_T \cdot \vec{q}_T}{(1+\xi)\,t} \tag{C.40}$$

$$v^{\pm} = \frac{1}{2(1-\xi)(\xi+1)^2 t^2}\Bigg\{ 8\xi\,(\Lambda\vec{\kappa}_T \cdot \vec{q}_T)^2$$
$$+ 2\Lambda\left(2\xi^2 + \xi - 1\right)t\,(X \pm 1)\,\vec{\kappa}_T \cdot \vec{q}_T$$
$$+ \left(\xi^2 - 1\right)t\left((\xi+1)(X \pm 1)^2 t - 4\Lambda\xi\kappa_T^2\right)\Bigg\}. \tag{C.41}$$

Powers of z_i-s are the same as in the vector case.

REFERENCES

[1] B. Pire, L. Szymanowski, Phys. Rev. **D** 71 (2005) 111501, [hep-ph/0411387]; J. P. Lansberg, B. Pire and L. Szymanowski, Phys. Rev. **D** 73 074014 (2006), [hep-ph/0602195].

[2] J.P. Lansberg, B. Pire, L. Szymanowski, 0709.2567 [hep-ph].

[3] B.C. Tiburzi, Phys. Rev. **D** 72 (2005) 094001, [hep-ph/0508112].

[4] A. Courtoy, S. Noguera, Phys. Rev. **D** 76 (2007) 094026, [0707.3366 [hep-ph]].

[5] E. Ruiz Arriola, W. Broniowski, Phys. Lett. **B** 649 (2007) 49, [hep-ph/0701243].

[6] M. Praszalowicz, A. Rostworowski, Phys. Rev. **D** 64 (2001) 074003, [hep-ph/0105188]; Phys. Rev. **D** 66 (2002) 054002, [hep-ph/0111196].

[7] S.-i. Nam, H.-C. Kim, A. Hosaka, M.M. Musakhanov, Phys. Rev. **D** 74 (2006) 014019, [hep-ph/0605259]; S. i. Nam and H. C. Kim, Phys. Rev. **D** 74 (2006) 096007, [hep-ph/0608018].

[8] M. Praszalowicz, A. Rostworowski, Acta Phys.Polon. **B** 34 (2003) 2699, [hep-ph/0302269].

[9] V.Yu. Petrov and P.V. Pobylitsa, hep-ph/9712203.

[10] V.Yu. Petrov, M.V. Polyakov, R. Ruskov, Ch. Weiss, K. Goeke, Phys. Rev. **D** 59 (1999) 114018, [hep-ph/9807229].

[11] C. V. Christov *et al.*, Prog. Part. Nucl. Phys. **37** (1996) 91 [hep-ph/9604441].

[12] W. Broniowski, B. Golli and G. Ripka, Nucl. Phys. **A** 703 (2002) 667 [hep-ph/0107139]; Phys. Lett. **B** 437 (1998) 24 [arXiv:hep-ph/9807261].

[13] A. Blotz, D. Diakonov, K. Goeke, N. W. Park, V. Petrov and P.V. Pobylitsa, Nucl. Phys. **A** 555 (1993) 765.

[14] A. V. Radyushkin, Acta Phys. Pol. **B** 30 (1999) 3647, [hep-ph/0011383].

[15] M.V. Polyakov, Ch. Weiss, Phys.Rev. **D** 59 (1999) 091502, [hep-ph/9806390]; Phys.Rev. **D** 60 (1999) 114017, [hep-ph/9902451].

[16] E. Ruiz Arriola, W. Broniowski, Phys.Rev. **D** 67 (2003) 074021, [hep-ph/0301202].

[17] R.M. Davidson, E. Ruiz Arriola, Acta Phys. Pol. **B** 33 1791 (2002), [hep-ph/0110291].

[18] H. Pagels and S. Stokar, Phys. Rev. D **20** (1979) 2947.

[19] J. S. Ball and T. W. Chiu, Phys. Rev. **D** 22 (1980) 2542.

[20] B. Holdom, J. Terning and K. Verbeek, Phys. Lett. **B** 232 (1989) 351; Phys. Lett. **B** 245 (1990) 612.

[21] R.D. Bowler, M. Birse, Nucl. Phys. **A** 582 (1995) 655, [hep-ph/9407336]; R.S. Plant, M. Birse, Nucl. Phys. **A** 628 (1998) 607, [hep-ph/9705372].

[22] M. R. Frank, K.L. Mitchell, C.D. Roberts and P.C. Tandy, Phys. Lett. **B** 359 (1995) 17 [hep-ph/9412219].

[23] W. Broniowski, in: Miniworkshop on Hadrons as Solitons, Bled 1999, hep-ph/9909438.

[24] A.E. Dorokhov, L. Tomio, Phys.Rev. **D** 62 (2000) 014016; I.V. Anikin, A.E. Dorokhov, L.Tomio, Phys. Lett. **B** 475 (2000) 361, [hep-ph/9909368].

[25] S.-i. Nam and H.-C. Kim, Phys. Rev. **D** 74 (2006) 076005, [hep-ph/0609267].

[26] S. Noguera, Int. J. Mod. Phys. **E** 16 (2007) 97, [hep-ph/0502171]; S. Noguera and V. Vento, Eur. Phys. J. **A** 28 (2006) 227, [hep-ph/0505102].

[27] A. Bzdak, M. Praszalowicz, Acta Phys. Polon. **B** 34 (2003) 3401, [hep-ph/0305217].

[28] M.M. Musakhanov, H.-C. Kim, Phys. Lett. **B** 572 (2003) 181, [hep-ph/0206233].

[29] D.I. Diakonov, V.Yu. Petrov, Nucl. Phys. **B** 245 (1984) 259; **B** 272 (1986) 457.

[30] D.I. Diakonov, V.Yu. Petrov, [hep-ph/0009006].

[31] M. Praszalowicz and G. Valencia, Nucl. Phys. **B** 341(1990) 27; E. Ruiz Arriola, Phys. Lett. **B** 253 (1991) 430.

[32] L. Ametller, L. Bergstrom, A. Bramon and E. Masso, Nucl. Phys. **B** 228 (1983) 301.

[33] J. Gronberg et al. (CLEO), Phys. Rev. D57, 33 (1998), [hep-ex/9707031].

[34] A. Courtoy and S. Noguera, arXiv:0804.4337 [hep-ph].

[35] W. Broniowski, E. R. Arriola and K. Golec-Biernat, Phys. Rev. **D** 77 (2008) 034023, [0712.1012 [hep-ph]].